

## Freezing/melting of Lennard-Jones fluids in carbon nanotubes

F. R. Hung and K. E. Gubbins

*Department of Chemical Engineering, North Carolina State University, Raleigh, North Carolina 27695*

R. Radhakrishnan

*Department of Chemistry and Courant Institute of Mathematical Sciences, New York, NY 10003*

K. Szostak and F. Béguin<sup>a)</sup>

*Centre de Recherche sur la Matière Divisée, CNRS-University, 45071 Orléans Cedex 02, France*

G. Dudziak and M. Sliwinska-Bartkowiak

*Institute of Physics, Adam Mickiewicz University, Umultowska 85, 61-614 Poznan, Poland*

(Received 13 August 2004; accepted 13 December 2004; published online 3 March 2005)

We report molecular simulation and experimental results for the freezing/melting behavior of Lennard-Jones fluids adsorbed in pores of cylindrical geometry, using simple models for multiwalled carbon nanotubes (MWNTs) of inner diameter 5 nm. For cylindrical pores, our results for a  $D=9.7\sigma_{ff}$  MWNT show no formation of regular three-dimensional crystalline structures. They also suggest that the outer layers experience an increase in the freezing temperature, while the inner layers provoke a depression in the freezing temperature with respect to the bulk freezing point. Dielectric relaxation spectroscopy shows a solid-fluid transition at 234 K for  $\text{CCl}_4$  in these MWNTs that is in qualitative agreement with that determined in our simulations for the inner adsorbed layers. © 2005 American Institute of Physics. [DOI: 10.1063/1.1862786]

Recent studies for pores of simple geometry have shown a rich phase behavior associated with freezing in confined systems.<sup>1–13</sup> The freezing temperature may be lowered or raised relative to the bulk freezing temperature, depending on the nature of the adsorbate and the porous material. In addition, new surface-driven phases may intervene between the liquid and solid phases in the pores. “Contact layer” phases of various kinds often occur, in which the layer of adsorbed molecules adjacent to the pore wall has a different structure from that of the adsorbate molecules in the interior of the pore. These contact layer phases have been predicted theoretically, and confirmed experimentally for several systems.<sup>4,9</sup> In addition, for some systems in which strong layering of the adsorbate occurs (e.g., activated carbon fibers), hexatic phases can occur; such phases have quasi-long-ranged orientational order, but positional disorder, and for quasi-two-dimensional systems occur over a temperature range between those for the crystal and liquid phases. These are clearly seen in molecular simulations, and recent experiments provide convincing evidence for these phases.<sup>14</sup> It has been shown that this apparently complex phase behavior results from a competition between the fluid-wall and fluid-fluid intermolecular interactions. For a given pore geometry and width, the phase diagrams for a wide range of adsorbates and porous solids can be classified in terms of a parameter  $\alpha$  which is the ratio of the fluid-wall to fluid-fluid attractive interaction.<sup>1,9,13</sup> In this letter we report molecular simulation studies of freezing in multiwalled carbon nanotubes (MWNTs). Simulations make use of the Landau–Ginzburg formalism for the free energy<sup>13</sup> and parallel tempering.<sup>15</sup> Experimental results from dielectric relaxation spectroscopy are reported for  $\text{CCl}_4$  in these materials.

In our experiments, we used high purity MWNTs prepared by catalytic decomposition of acetylene on a Co/MgO

solid solution catalyst, according to the process described in Ref. 16. The MWNTs were opened according to the procedure described in Ref. 17, using an excess of boiling concentrated nitric acid during 30 min under continuous stirring at 140 °C. The resulting material is recovered by filtration and washed several times with demineralized water until neutral pH. Since it contains debris produced during the acid oxidation of the tips, it is then treated by carbon dioxide at 525 °C during 60 min, in order to oxidize selectively these disordered carbon nanostructures, while keeping the MWNTs intact.<sup>17</sup>

Transmission Electron Microscopy (TEM, Philips CM 20) of the MWNTs material after the two-step oxidation treatment shows that all tips are efficiently opened. Higher magnification reveals that the average outer diameter of the nanotubes slightly decreased from 10 to 15 nm for the pristine nanotubes to 8–12 nm, without destruction of the walls, i.e., keeping perfectly continuous outer layers. The histogram of the inner diameters shows a good calibration of the central canal, with values mostly in the narrow range from 4 to 5 nm.

The nitrogen adsorption isotherms of the pristine MWNTs and of MWNTs after the opening process are presented in Fig. 1. Both isotherms are of type IV, characteristic of a mesoporous material. However, in the case of the opened nanotubes, the total adsorbed volume close to  $P/P_0 = 1$  is much higher than for the pristine nanotubes, confirming the contribution of the central canal to adsorption after removal of the tips. The Brunauer–Emmett–Teller specific surface area increases from 220 m<sup>2</sup> for the pristine nanotubes to 310 m<sup>2</sup>/g for the opened nanotubes, and the mesopore volume from 0.99 cm<sup>3</sup>/g to 1.54 cm<sup>3</sup>/g.

We performed grand canonical Monte Carlo (MC) simulations of Lennard-Jones (LJ) fluids adsorbed in cylindrical pores of diameter  $D$  using the potential due to Peterson, Walton, and Gubbins.<sup>18</sup> Systems of up to 64 000 molecules were considered. We calculated the Landau free energy as a function of an effective bond orientational order parameter  $\Phi$ ,

<sup>a)</sup> Author to whom correspondence should be addressed; electronic mail: [beguin@cnrs-orleans.fr](mailto:beguin@cnrs-orleans.fr)

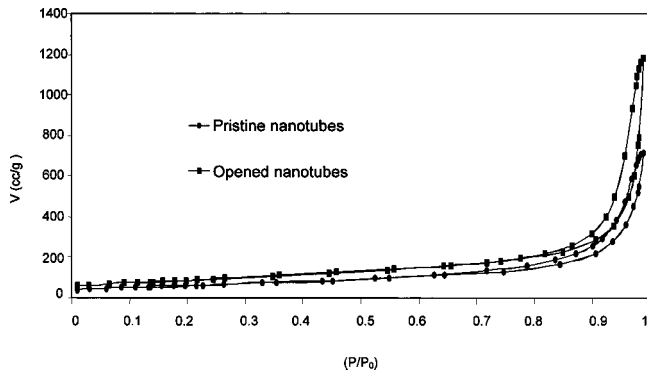


FIG. 1. Comparative nitrogen adsorption isotherms at 77 K on pristine and opened MWNTs.

which is sensitive to the degree of order in the system. The Landau free energy approach used in earlier studies<sup>3,19</sup> was extended to incorporate spatial inhomogeneity in the order parameter, and a generalized Landau–Ginzburg approach was developed to determine the Landau free energy surface of inhomogeneous fluids,<sup>13</sup> with the latter given by

$$\Lambda[\Phi(\mathbf{r})] = -k_B T \ln(P[\Phi(\mathbf{r})]) + \text{constant}, \quad (1)$$

where  $k_B$  is the Boltzmann constant,  $T$  is the temperature, and  $P[\Phi(\mathbf{r})]$  is the probability of observing a system having an order parameter value between  $\Phi$  and  $\Phi + \delta\Phi$  at the position given by  $\mathbf{r}$ . The probability distribution function  $P[\Phi(\mathbf{r})]$  was determined during the simulations using umbrella sampling in pores of slit-like geometry,<sup>13</sup> and parallel tempering<sup>15</sup> for pores of cylindrical geometry. We found significant ordering into distinct molecular layers in the systems considered; therefore it is possible to define the order parameter  $\Phi(\mathbf{r})$  using a two-dimensional bond orientational order parameter, defined as<sup>13</sup>

$$\Phi(\mathbf{r}) = \sum_{j=1}^n \frac{\left| \int d\rho \Psi_{6,j}(\rho) \right|}{\int d\rho} \delta(\mathbf{r} - \hat{\mathbf{r}}_j); \quad (2)$$

$$\Psi_{6,j}(\rho) = \frac{1}{N_b} \sum_{k=1}^{N_b} \exp(i6\theta_k),$$

where the first sum is over the adsorbed molecular layers and  $\hat{\mathbf{r}}_j$  is the coordinate of the plane in which molecules in layer  $j$  are most likely to lie on. We expect  $\Phi(\mathbf{r})=1$  for two-dimensional hexagonal crystals and  $\Phi(\mathbf{r})=0$  for two-dimensional liquids.  $\Psi_{6,j}(\rho)$  measures the hexagonal bond order at position  $\rho$  within each two-dimensional layer  $j$ .  $N_b$  is the number of nearest neighbors of a molecule at position  $\rho$  and  $\theta_k$  is the orientation of each nearest neighbor bond with respect to an arbitrary axis.<sup>13</sup> For cylindrical pores, a quasi-two-dimensional configuration of each molecular layer can be obtained by cutting each one of the concentric layers along the axial direction and unrolling it flat. The grand free energy of a particular phase is then related to the Landau free energy by<sup>13</sup>

$$\exp(-\beta\Omega) = \int d\Phi \exp(-\beta\Lambda[\Phi(\mathbf{r})]). \quad (3)$$

The probability distribution function  $P[\Phi(\mathbf{r})]$  was determined during the simulations using parallel tempering<sup>15</sup> for

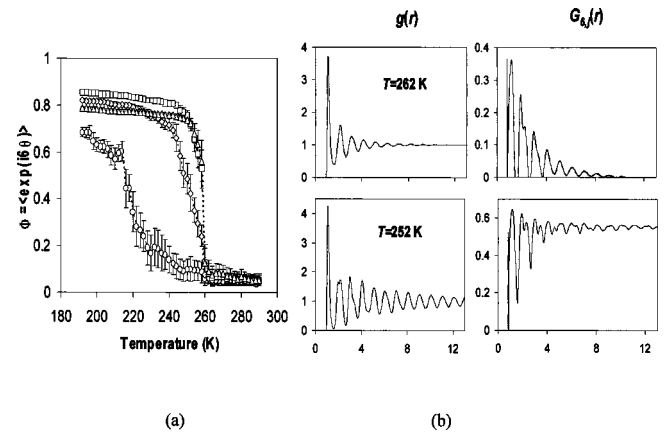


FIG. 2. (a) Two-dimensional, bond orientational order parameter average values in the molecular fluid layers of LJ  $\text{CCl}_4$  confined in a MWNT of diameter  $D=9.7\sigma_{ff}$  (5 nm). Triangles, squares, diamonds, and circles represent the order parameter values for the contact, second, third, and fourth layers, respectively. The dotted line represents the bulk solid–fluid transition temperature. (b) Positional and orientational pair correlation functions in the unwrapped contact layer of LJ  $\text{CCl}_4$  confined in a MWNT of diameter  $D=9.7\sigma_{ff}$  (5 nm) showing liquid phase at  $T=262$  K and crystal phase at  $T=252$  K.

pores of cylindrical geometry. The method of parallel tempering is a Monte Carlo scheme that has been derived to achieve good sampling of systems that have a free energy landscape with many local minima.<sup>20</sup> Yann and de Pablo<sup>15</sup> implemented this scheme in the grand canonical ensemble, performing a MC simulation in  $n$  systems which differ in both temperature and chemical potential. In addition to the standard MC trial moves, they proposed configuration swaps in this method. A swap attempt between configurations  $i$  and  $j$  is accepted with probability given by

$$p_{\text{acc}}(x_i \leftrightarrow x_j) = \min[1, \exp(\Delta\beta\Delta U - \Delta(\beta\mu)\Delta N)], \quad (4)$$

where  $\Delta\beta=1/k_B T_i - 1/k_B T_j$ , and  $\Delta U$  and  $\Delta N$  are the difference in potential energies and number of particles, respectively, between configurations  $i$  and  $j$ . We have used as many as 50 different configurations in our calculations with the parallel tempering Monte Carlo scheme, to cover all the phase space of interest and to guarantee frequent swaps between replicas. We have checked the evolution of the parallel tempering simulation as a function of Monte Carlo steps and, after the equilibration, we verified that each configuration visited many sets of  $(T, \mu)$  along a single simulation run. The nature of the phases in each molecular layer was determined by measuring the two-dimensional bond orientational order parameter and by monitoring the two-dimensional, in-plane positional and orientational pair correlation functions within each layer. The positional pair correlation function in layer  $j$  is given by the familiar radial distribution function  $g_j(\rho)$ , measured within the two-dimensional plane formed by each layer  $j$ . The orientational pair correlation function is given by  $G_{6,j}(\rho) = \langle \Psi_j^*(0) \Psi_j(\rho) \rangle$ .

The method described above has been used to study the freezing behavior of LJ  $\text{CCl}_4$  adsorbed in model MWNTs of internal diameter  $D=5$  nm ( $D^*=9.7$ ). The formation of five concentric layers of adsorbate was observed when the confined fluid solidified. In Fig. 2(a) we show the average values of the two-dimensional, bond orientational order parameter in the individual layers, as a function of temperature. We observe a discontinuity in the average order parameters of the contact and second layers around 260 K, suggesting a

phase transition in these two layers. The change in the order parameter for the third layer is less abrupt than in the first two layers and starts around 255 K. In the fourth layer, the order parameter value increases continuously until it jumps around 215 K, reaching a maximum value of  $\Phi \sim 0.7$  at lower temperatures. Our results suggest that for this specific pore diameter, the contact and first inner layers freeze at temperatures higher than the bulk freezing point, whereas the inner layers experience a depression in the freezing temperature when compared to that of the bulk. These observations are corroborated by our results for the positional and orientational pair correlation functions in the unwrapped layers. Some of our results for the contact layer are shown in Fig. 2(b). At  $T=262$  K, the isotropic positional pair correlation function and the exponential decay in the orientational pair correlation function are signatures of an isotropic liquid. At  $T=252$  K, the features observed in both pair correlation functions are characteristic of a two-dimensional hexagonal crystal. Similar features were found for the other layers.

Our results for the  $D=9.7\sigma_{ff}$  MWNTs did not show any sign of ordering of the confined LJ  $\text{CCl}_4$  into regular, three-dimensional (3D) crystal structures. This finding is in agreement with previous simulation<sup>10</sup> and experimental<sup>10,21</sup> studies, where it was shown that for pore diameters below  $20\sigma_{ff}$  only partial crystallization occurs. The same studies found that for silica materials, the lower limit below which there are no 3D crystal domains in the system was around  $D=12\sigma_{ff}$ .<sup>10,20</sup> Our simulations for carbon nanotubes of smaller diameters show that the freezing temperatures increase as the pore diameter decreases.

The freezing of  $\text{CCl}_4$  confined in MWNTs has been investigated by dielectric relaxation spectroscopy as described elsewhere.<sup>10–13,22</sup> The experimental setup consisted of a parallel plate capacitor of empty capacitance  $C_0$ . The capacitance  $C$  and the tangent loss,  $\tan(\delta)$ , of the capacitor filled with the sample were measured at different temperatures and frequency range from 10 Hz–1 MHz, using Solartron 1260 Impedance Analyzer. A suspension of opened MWNTs in the pure adsorbate ( $\text{CCl}_4$ ) was introduced between the capacitor plates. A similar measurement was performed for the sample of closed MWNTs, where  $\text{CCl}_4$  was not adsorbed inside the nanotubes. The relative permittivity is related to the measured quantities by  $\kappa_r=C/C_0$ ,  $\kappa_i=\tan(\delta)/\kappa_r$ , where  $\delta$  is the angle by which current leads the voltage.

Figure 3 shows the capacity  $C$  as a function of temperature for  $\text{CCl}_4$  confined in the opened MWNTs with average internal canal diameter of 5 nm. Since the sample studied is a suspension of  $\text{CCl}_4$ -filled carbon nanotubes in pure  $\text{CCl}_4$ , the signal contains both contributions of bulk and confined  $\text{CCl}_4$ . The feature observed at  $T=250$  K in the capacity  $C$  vs temperature plot was found at the same temperature for  $\text{CCl}_4$  adsorbed on the pristine MWNTs. Since the latter are essentially closed, this discontinuity is associated with the melting point of bulk  $\text{CCl}_4$ . By contrast, the sharp increase at  $T=234$  K in Fig. 3 is attributed to melting in the pores. The features found at  $T=205$  K and  $T=172$  K may be associated with a solid-solid transition, since such a transition (from monoclinic to rhombohedral crystal) occurs in bulk  $\text{CCl}_4$ .

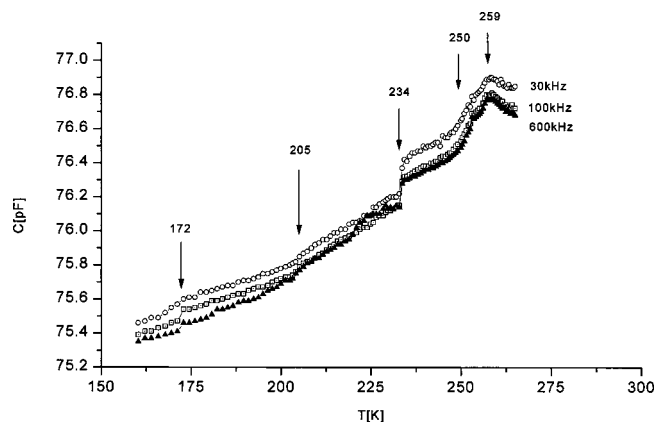


FIG. 3. Dependence of capacity  $C$  with temperature for  $\text{CCl}_4$  in open MWNTs with average pore diameter of 5 nm (average external diameter: 10 nm), from dielectric relaxation spectroscopy. The results were obtained at 30 kHz (circles); 100 kHz (squares); 600 kHz (triangles). The signals are for both bulk and confined  $\text{CCl}_4$ .

The melting temperature measured in this experiment for confined  $\text{CCl}_4$  is in qualitative agreement with the value found in our simulations for the inner layers. Hence, we can conclude that for this specific cylindrical pore diameter (5 nm), the inner layers experience a depression in the freezing temperature when compared to that of the bulk.

- <sup>1</sup>L. D. Gelb, K. E. Gubbins, R. Radhakrishnan, and M. Sliwinska-Bartkowiak, *Rep. Prog. Phys.* **62**, 1573 (1999).
- <sup>2</sup>M. Miyahara and K. E. Gubbins, *J. Chem. Phys.* **106**, 2865 (1997).
- <sup>3</sup>R. Radhakrishnan and K. E. Gubbins, *Mol. Phys.* **96**, 1249 (1999).
- <sup>4</sup>M. Sliwinska-Bartkowiak, J. Gras, R. Sikorski, R. Radhakrishnan, L. D. Gelb, and K. E. Gubbins, *Langmuir* **15**, 6060 (1999).
- <sup>5</sup>H. Dominguez, M. P. Allen, and R. Evans, *Mol. Phys.* **96**, 209 (1998).
- <sup>6</sup>K. Kaneko, A. Watanabe, T. Iiyama, R. Radhakrishnan, and K. E. Gubbins, *J. Phys. Chem. B* **103**, 7061 (1999).
- <sup>7</sup>A. Watanabe and K. Kaneko, *Chem. Phys. Lett.* **305**, 71 (1999).
- <sup>8</sup>R. Radhakrishnan, K. E. Gubbins, A. Watanabe, and K. Kaneko, *J. Chem. Phys.* **111**, 9058 (1999).
- <sup>9</sup>R. Radhakrishnan, K. E. Gubbins, and M. Sliwinska-Bartkowiak, *J. Chem. Phys.* **112**, 11048 (2000).
- <sup>10</sup>M. Sliwinska-Bartkowiak, G. Dudziak, R. Sikorski, R. Gras, R. Radhakrishnan, and K. E. Gubbins, *J. Chem. Phys.* **114**, 950 (2001).
- <sup>11</sup>M. Sliwinska-Bartkowiak, G. Dudziak, R. Sikorski, R. Gras, K. E. Gubbins, and R. Radhakrishnan, *Phys. Chem. Chem. Phys.* **3**, 1179 (2001).
- <sup>12</sup>M. Sliwinska-Bartkowiak, R. Radhakrishnan, and K. E. Gubbins, *Mol. Simul.* **27**, 323 (2001).
- <sup>13</sup>R. Radhakrishnan, K. E. Gubbins, and M. Sliwinska-Bartkowiak, *J. Chem. Phys.* **116**, 1147 (2002).
- <sup>14</sup>R. Radhakrishnan, K. E. Gubbins, and M. Sliwinska-Bartkowiak, *Phys. Rev. Lett.* **89**, 076101 (2002).
- <sup>15</sup>Q. Yann and J. J. de Pablo, *J. Chem. Phys.* **111**, 9509 (1999).
- <sup>16</sup>S. Delpoux, K. Szostak, E. Frackowiak, S. Bonnamy, and F. Béguin, *J. Nanosci. Nanotechnol.* **2**, 481 (2002).
- <sup>17</sup>S. Delpoux, K. Szostak, E. Frackowiak, and F. Béguin, *Chem. Phys. Lett.* (to be published).
- <sup>18</sup>B. K. Peterson, J. P. R. B. Walton, and K. E. Gubbins, *J. Chem. Soc., Faraday Trans. 1* **82**, 1789 (1986).
- <sup>19</sup>R. M. Lynden-Bell, J. S. van Duijneveldt, and D. Frenkel, *Mol. Phys.* **80**, 801 (1993).
- <sup>20</sup>D. Frenkel, B. Smit, *Understanding Molecular Simulation: From Algorithms to Applications*, 2nd ed. (Academic, London, 2002).
- <sup>21</sup>D. Morineau, G. Dosseh, C. Alba-Simionesco, and P. Llewellyn, *Philos. Mag. B* **79**, 1847 (1999).
- <sup>22</sup>A. Chelkowski, *Dielectric Physics* (Elsevier, North-Holland, New York, 1980).